https://doi.org/10.5194/egusphere-2026-5527
Preprint. Discussion started: 23 September 2026

A Decade of Synchronous Ice Speed Change Across Central & Southeast Greenland

Mae E. Evans[1*], Anna E. Hogg[1], Trystan Surawy-Stepney[1], Benjamin J. Wallis[1], Ross A. W. Slater [1], Richard Rigby[1]

[1] School of Earth, Environment & Sustainability, University of Leeds, Leeds, LS2 9JT, United Kingdom

Correspondence to: Mae Evans (mn19mee@leeds.ac.uk)

Abstract. Marine-terminating glaciers in central and southeast Greenland are major contributors to Greenland's mass loss making it essential to monitor their changing behaviour. Here, we use over a decade of Sentinel-1 satellite observations to measure the change in ice speed on 66 glaciers between 2014 and 2025. We observe widespread, synchronous acceleration between 2016 and 2020, during which two thirds of glaciers accelerate and 6 more than double their velocity, with many glaciers reaching their fastest speeds since at least 2000. This period is followed by widespread deceleration after 2020, although the slowdown is smaller in magnitude and more gradual, with most glaciers remaining faster than their pre-2016 values. The acceleration coincides with exceptionally warm surface ocean waters in 2016 (+3 °C anomaly), warming at depth in 2018 (+1 °C anomaly) and a prolonged reduction in regional sea-ice concentration, suggesting ocean-driven processes played a role in driving this change. Our results show that ice dynamic change in southeast Greenland has been more spatially extensive and larger magnitude than previously recognised, highlighting the sensitivity of these glaciers to environmental forcing and their susceptibility to rapid, synchronous change.

1 Introduction

Over the 28-year period from 1992 to 2020, the Greenland Ice Sheet experienced a significant negative mass balance, losing 4,892 ± 457 Gt of ice at an average rate of 169 ± 16 Gt per year (Otosaka et al., 2023). The 13.5 mm Greenland contributed to global sea levels over this same time-period accounted for 65 % of the ice sheet contribution to sea level rise (Fox-Kemper et al., 2023). Ice dynamics are a major driver of this mass loss and are projected to remain so in the future (Choi et al., 2021). Since the 1970s, increases in the rate of calving and ice discharge above steady-state levels have contributed around two-thirds of the ice sheet's total mass loss (Mouginot et al., 2019a). In more recent decades, this fraction has declined to just under half (King et al., 2020; Shepherd et al., 2020) as negative surface mass balance associated with atmospheric warming has become more dominant (van den Broeke et al., 2016; Mouginot et al., 2019a). Nevertheless, dynamic losses have increased in absolute terms, and total mass loss has accelerated since the 1990s (Otosaka et al., 2023).

Mass loss due to ice dynamics is particularly pronounced in regions with many fast-flowing marine-terminating glaciers, such as the west, northwest and southeast Greenland (Mouginot et al., 2019a). Southeast Greenland, in particular, accounted for

https://doi.org/10.5194/egusphere-2026-5527
Preprint. Discussion started: 23 September 2026

around a third of Greenland's total ice discharge between 1986 and 2017; equal to the combined output of the north, northeast and southwest regions (Mankoff et al., 2020; Mouginot et al., 2019a). Discharge from southeast Greenland changed little through the 1980s and 1990s before increasing in the early 2000s as several major glaciers, including Helheim, retreated and accelerated (Howat et al., 2007; King et al., 2020; Mankoff et al., 2020). Regional discharge increased by 18 %, peaking in 2005 and then undergoing little change until 2016 (King et al., 2020). The central east coast showed similar behaviour, mainly driven by Kangerlussuaq Glacier, which also reached maximum retreat and acceleration in 2005 before levelling off until 2016 (Bevan et al., 2019; Brough et al., 2019; Enderlin et al., 2014; Mankoff et al., 2020). These changes have been linked to warming of the Atlantic Water ocean layer (Seale et al., 2011; Straneo and Heimbach, 2013), which, due to the deep fjords typical of this region was able to reach the glacier fronts and interact directly with grounded ice (Wood et al., 2021).

A study of 24 glaciers in central east Greenland found multiyear calving front retreat between 2016 and 2019 (Brough et al., 2023), including at Kangerlussuaq Glacier (Bevan et al., 2019; Brough et al., 2019). This retreat has been linked to warming surface waters that weakened the rigid mélange and enhanced iceberg calving (Brough et al., 2019, 2023), highlighting the important role buttressing plays in modulating calving frequency and ice dynamic processes. Calving front retreat was also observed in 2016 on peripheral glaciers along the southeast coast. However, in this case, change was attributed to increased surface meltwater driven by atmospheric warming which increased submarine melting at the glacier front (Liu et al., 2022). In 2018, Steenstrup Glacier accelerated by around 300 %, coinciding with a warm Atlantic water anomaly in its fjord (Chudley et al., 2023), providing further observational evidence of strong dynamic response to ocean forcing at the scale of one ice stream. Although recent studies have identified isolated episodes of dynamic change along Greenland's CE and SE coast in the late 2010s, this work has focussed either on individual glaciers or on smaller sections of the coastline. This motivates the need for a more spatially comprehensive and temporally extended assessment of change.

Here, we measure change in ice speed at high temporal resolution on 66 marine-terminating glaciers along Greenland's central and southeast coasts, over the past decade from 2014 to 2025. We identify a widespread episode of ice speed acceleration and then deceleration which has significant implications for the region's sea level contribution. We analysed ocean temperature and atmospheric datasets to better understand the environmental drivers of change in the region.

2 Methods

2.1 Ice velocity measurements

We measured ice speed across the central east (CE) and southeast (SE) drainage basins (Mouginot et al., 2019b) of the Greenland Ice Sheet over an 11-year period, from October 2014 to August 2025 using data from the Sentinel-1 synthetic aperture radar (SAR) satellites. We used all available unique sequential pairs of Interferometric Wide (IW) swath, single-look complex (SLC) images acquired by Sentinel-1A, -1B, and -1C during the study period, with temporal baselines of either 6 or 12-days for each pair reflecting the repeat cycle of the satellites. We measured ice speed using the intensity feature tracking

https://doi.org/10.5194/egusphere-2026-5527
Preprint. Discussion started: 23 September 2026

method (Strozzi et al., 2002a) and the GAMMA Remote Sensing software, following cross-correlation methods that identify stable intensity patterns between repeat acquisitions (Selley et al., 2021; Strozzi et al., 2002b). We take the signal-to-noise-ratio (SNR) weighted mean of tracking results from three combinations of window and step sizes in range / azimuth (256 × 64, 40 × 10; 350 × 76, 80 × 16; 512 × 128, 80 × 20) (Davison et al., 2024; Lemos et al., 2018; Selley et al., 2021; Wallis et al., 2023b), and use the Arctic DEM v4.1 (Porter et al., 2023) to convert offsets into ground displacement. We compared our ice speed measurements with a reference ice speed map consisting of annually averaged Greenland Ice Sheet surface velocity measurements derived from Sentinel-1 for Oct 1st 2019 - Sept 30th 2020 from the Copernicus Climate Change Service (Copernicus Climate Change Service, Climate Data Store, 2020; Nagler et al., 2015), removing outliers based on both flow direction (deviations > 45° for velocities > 50 m yr^{-1} removed) and velocity magnitude (over 5 times greater or 0.1 times smaller removed) (Wallis et al., 2023a). Our ice speed data was then aggregated by the mid-date between the primary and secondary image acquisition dates and mosaicked onto to a 100 m x 100 m grid. The average ice speed map was generated by averaging the full set of these primary/secondary image date-pair mosaics.

2.2 Ice velocity error

Several main sources contribute to uncertainty in ice velocity measurements including, i) error in the coregistration of the SAR image pairs during the cross-correlation step (Lemos et al., 2018); ii) error in the DEM caused by ice surface elevation change which affects georeferencing accuracy; iii) atmospheric effects such as ionospheric disturbances (Nagler et al., 2015); iv) uncertainty caused by variations in the radar penetration depth between wet and dry snow conditions (Rott et al., 2020; Wallis et al., 2023b); v) inaccuracies in the cross-correlation peak-finding algorithm; and vi) broadening of the cross-correlation peak due to loss of image information between acquisitions (Bhattacharya et al., 2018). We generate a pixel-wise, spatially variable error estimate for each velocity map by scaling the signal-to-noise ratio (SNR) of the cross-correlation peak with the ice speed (Lemos et al., 2018). This method produces a spatially and temporally variable error field which is directly related to the cross-correlation measurement technique (Fig. S3).

Additional uncertainty arises from gaps in the spatial coverage of the ice velocity measurements and the density of these observations obtained throughout the study period. To assess this, we measured the number of successful velocity measurements at each pixel across the study region (Fig. S4). The southeast region of Greenland experiences frequent heavy snowfall, which can limit the success of offset-tracking technique and therefore reduce measurement density (Solgaard et al., 2021), however, despite this we achieve robust coverage across much of the coastline, with more than 500 successfully tracked velocity observations on most outlet glaciers during the 11-year study period (Fig. S4). Coverage decreases notably inland (<100 observations), but these areas do not contain the faster-flowing glaciers that are most susceptible to change which are the focus of this study. In contrast, there is more limited coverage in the northern CE coastline, where four glaciers (Bredegeltsjer, Dendrit, Apuseeq An, and Sortebrae) have only 30-50 velocity measurements per glacier over the 10-year period caused by relatively few Sentinel-1 IW-mode acquisitions.

2.3 Ice speed timeseries

Ice speed time series were generated pixelwise by temporally stacking the date-pair mosaics and then filtered to remove outliers using two filtering steps based on an outlier-robust estimate of the standard deviation. The outlier-robust standard deviation (ORSD) is approximated by scaling the median absolute deviation (MAD) by 1.4826. First the ORSD is calculated with respect to the full time series, and data points which are > 3 ORSD from a 1-year rolling median are removed. Secondly, a Hampel filter with a rolling-window size of 90 observations is applied to the remaining data. In the Hampel filter, any observations > 2 ORSD from the median of the window are removed, with the ORSD recalculated in each window. This filtering was applied to the x and y components of velocity, to better mask magnitude values where there was a large anomaly in a single component. We also removed any ice speed measurements with erroneously large error values (greater than 1×10^{30} m/yr). Rates of ice speed change (trends) were calculated on a pixelwise basis over the full date range by fitting a linear trend through the filtered velocity time series in each pixel.

We extracted individual ice speed time series on 66 outlet glaciers in the CE and SE regions of the Greenland Ice Sheet. For each glacier, ice speed was sampled within a 1 km × 1 km box positioned ~1.5 km inland of the most retreated calving front location (CFL), with CFL's measured using our own manually derived observations (see Terminus Position section) or taken from other freely available datasets (Black and Joughin, 2022). For each glacier, we calculated the average ice speed and associated error in the sampling box at every timestep. We produced an error-weighted smoothed, daily estimate of ice speed and ice speed error using a Kalman Smoother (Wallis et al., 2023b), which are the primary time series used in all subsequent analyses. When calculating speed changes between two months (Fig. 2 and 3), we resampled the daily time series to monthly resolution by averaging the ice speed and associated error within each month. When averaging the uncertainty here, and across the sampling box over the glacier, we assume perfect covariance between measurements, resulting in the most conservative estimate of the uncertainty. For derived quantities such as the percent change in ice speed between two months (Fig. 3), errors were propagated by adding in quadrature. We applied a 12-month rolling mean to the Kalman smoothed ice speed time series when plotting data on the 'highlight glaciers' (Fig. 2), and extended the record of ice speed measurements prior to 2014 using annual ice velocity estimates from ITS LIVE (Gardner et al., 2024) using the same sampling box. ITS LIVE ice velocity fields are produced from mosaics that combine optical (Landsat) and SAR imagery.

2.4 Terminus position

We measured change in calving front location (CFL) on 15 highlight glaciers (Fig. 1). Between 2015 and 2021 we used the Black and Joughin (Black and Joughin, 2022) dataset, and extended this record from January 2022 to September 2024 by manually delineating terminus positions in Sentinel-1 imagery using the GEEDiT digitisation tool (Lea, 2018). We generated a monthly time series by using the first available Sentinel-1 acquisition in each month. If that image was obscured, we used the next suitable acquisition. After digitisation, we quantified terminus position change using the curvilinear box method implemented in MaQiT (Lea, 2018). Although we performed digitisation at the spatial resolution of the SAR imagery (±10 m), the uncertainty associated with manual delineation is typically ~25 m and may be larger for heavily crevassed termini or for tidewater glaciers influenced by mélange or sea ice (Black and Joughin, 2023).

2.5 Environmental forcing data

We extracted environmental forcing data from the region shown in Fig. 1a, which spans the continental shelf along CE and SE Greenland on the ocean side and the full extent of the fast-flowing glacier regions on the land side. We took ocean temperature from the Arctic Ocean Physics Reanalysis product from the Copernicus Marine Environment Monitoring Service (Arctic Ocean Physics Reanalysis, 2025). For 2 meter air temperature we used ERA5 reanalysis data (Copernicus Climate Change Service, 2023), and sea-ice concentration was taken from the Arctic Ocean Sea Ice Reanalysis (Arctic Ocean Sea Ice Reanalysis, 2025), also from the Copernicus Marine service. For all variables, we computed spatial averages across the full region. Anomalies were calculated relative to the mean over the full period 1991–2024 (1993–2024 for sea-ice concentration).

https://doi.org/10.5194/egusphere-2026-5527
Preprint. Discussion started: 23 September 2026

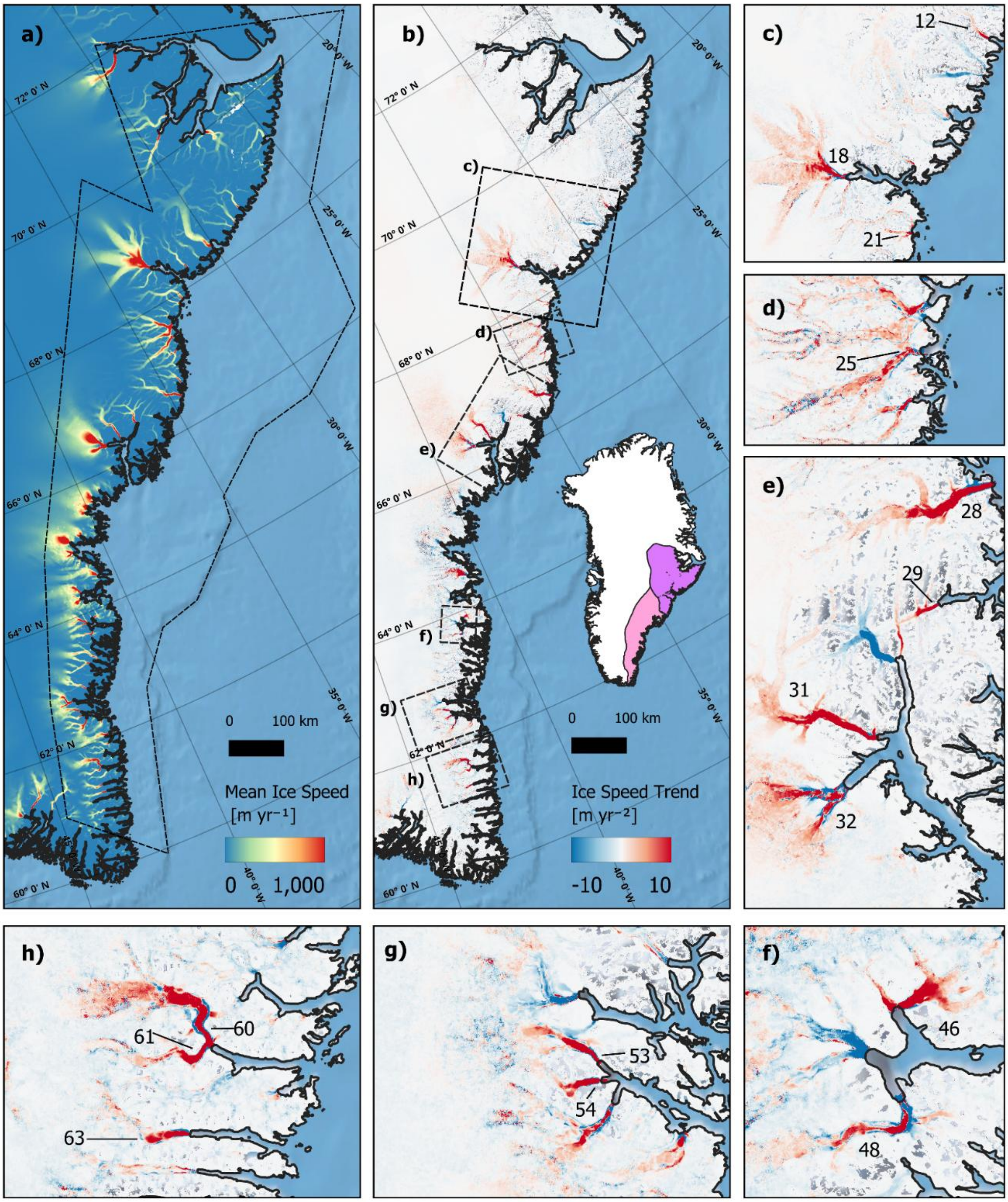

Figure 1 | Ice speed and speed change trends across central east and southeast Greenland. a) Mean ice speed (m yr^{-1}) for the central east and southeast Greenland study region from October 2014 to August 2025. The black dashed line marks the boundary of the area used to extract ocean and atmospheric

https://doi.org/10.5194/egusphere-2026-5527
Preprint. Discussion started: 23 September 2026

forcing data in Fig. 4. b) Pixelwise trends in ice speed over the same period with speedup (red) and slowdown (blue) shown. The inset map of Greenland shows the central east (purple) and southeast (pink) drainage basins from Mouginot et al. 2019 (Mouginot et al., 2019a), with the locations of zoomed panels in Fig. 1c–h also noted (black dashed boxes). These regions focus on selected highlight glaciers where velocity time series are shown in Fig. 2. c–h) Zoomed maps of ice-speed trends for individual highlight glaciers, labelled by glacier ID: c) Borggraven (12), Kangerlussuaq (18), Apuliliip Apusiia (Polaric) S (21). d) Unartit (25). e) K.J.V. Steenstrup Nørdre Bræ (28), Kattilersorpia (Glacier de France) (29), Apuseerajik (Fenris) (31), Helheim (32). f) Sleipner (46), Storebjørn (48). g) Mogens Heinesen N (53), Mogens Heinesen C (54). h) Anorituup Kangerlua CN (60), Anorituup Kangerlua CS (61), Avaqqat Kangerluat (63). The black coastline is from Gerrish (2020) (Gerrish, 2020) .

3 Results

3.1 Spatial patterns of ice speed change

To identify the broad spatial pattern and magnitude of dynamic change across central east (CE) and southeast (SE) Greenland over the past decade, we first examine the mean ice speed and ice speed trends derived from the full Sentinel-1 record (Fig. 1). Ice flow in this region is dominated by fast-flowing outlet glaciers terminating in long, narrow fjord systems. Kangerlussuaq and Helheim are the fastest glaciers in the region, reaching speeds of over 8 km yr^{-1} near their terminus. In contrast, several smaller outlet glaciers flow at only ~300 m yr^{-1}. Fast flow (>1 km yr^{-1}) can extend up to 50 km inland on the region's largest outlet glaciers but is generally confined to within 10 km of the termini on slower glaciers.

Ice speed trends were measured by applying a linear fit to the full Sentinel-1 ice velocity record from 2014 to 2025, on every pixel in the study region (Fig. 1b). We find that non-zero trends are almost entirely restricted to the outlet glaciers, with minimal rates of change inland. On these glaciers, the strongest trends (greater than 50 m yr^{-2}) are located near the glacier termini. Exceptions to this include K.J.V Steenstrup and Apuseerajik (Fenris) glaciers, in which large trends can be seen over distances greater than 30 km upstream of the terminus (Fig. 1e). Positive trends dominate much of the CE coast south of 69°N, with Boggraven, Kangerlussuaq and K.J.V Steenstrup reaching approximately 60, 110 and 400 m yr^{-2}, respectively (Fig. 1c, e). Similar positive trends are observed across much of the SE coast. Here, Mogens Heinsen N and C glaciers show trends exceeding 100 m yr^{-2} near their termini (Fig. 1g), while Anorituup Kangerlusa CN and CS reach values above 200 m yr^{-2} (Fig. 1h). However, neighbouring glaciers can show contrasting behaviour within the same fjord system. Helheim and Apuseerajik (Fenris) Glaciers both show strong acceleration, with Apuseerajik (Fenris) exceeding 300 m yr^{-2}, whereas neighbouring Nigertiip Apusiia (Midgård) shows a negative trend of nearly –200 m yr^{-2} (Fig. 1e). Similarly, A.P. Bernstorff and Sleipner Glaciers display opposing trends with negative and positive velocity changes respectively (Fig. 1f). Overall, these trends demonstrate that substantial dynamic change is widespread across CE and SE Greenland. However, since linear trends can obscure when these changes occurred, we next examine the temporal evolution of glacier speed to further investigate the timing and magnitude of speed changes.

3.2 Widespread, synchronous acceleration and deceleration

To better understand the timing of the ice speed change in central and southeast Greenland, we extracted time series of ice speed on all glaciers in the study region (Fig. 2, Fig. S1). These data reveal a widespread, multi-year acceleration of glaciers along the whole length of the CE and SE Greenland coast initiating between January and June 2016 and persisting until 2020. This was followed by a peak in speeds and deceleration from 2020 until the end of the study period. We expand upon each of these phases in the next three sections.

3.2.1 Acceleration phase (2016-2020)

During the period 2016-2020, 43 out of the 66 glaciers (65 %) experienced a significant increase in ice velocity, 7 slowed and 16 showed no significant change (Fig. 2, Fig. 3a). Figure 2 shows timeseries of ice velocity on the 15 glaciers with the most pronounced ice speed change over the full study period from 2016 to 2024. We refer to these glaciers from here on as "highlight" glaciers, with time series for all 66 glaciers in the study region shown in Figure S1. These time series show the very large magnitude change in ice speed that occurred in just a few years. The largest percent increases in ice speed in this four year time period, occurred on K.J.V Steenstrup (Fig. 2e) which increased from 1466.7 ± 116 km m yr^{-1} to 4660.2 ± 74 m yr^{-1} (+217.7 ±26 %), Kattilersorpia (Glacier de France) (Fig. 2f) which increased from 426.0 ± 31 m yr^{-1} to 951.2 ± 20 m yr^{-1} (+123.3 ± 17 %), Apuseerajik (Fenris) which increased in speed from 1750.6 ± 94 m yr^{-1} to 3711.2 ± 75.1 m yr^{-1} (+112.0 ± 12 %) (Fig. 2g) and Sortebrae which is a surge type glacier with a 167 ± 45 % increase from 179.9 ± 28 m yr^{-1} to 480.8 ± 32 m yr^{-1}. The largest slowdown during this period occurred on Nigertiip Apusiia (Midgård) and Dendrit Glaciers (−15.6 ± 4 % and −11.8 ± 7 %, respectively) which were the only two glaciers to decrease in speed by more than 10 %. Overall, accelerating glaciers increased their speed by 43.1 % on average, while those that decelerated slowed by an average of 9 %, and in total six glaciers more than doubled their speed during this period (Sortebrae, Apuliliip Apusiia (Polaric) S, K.J.V Steenstrup, Kattilersorpia (Glacier de France), Apuseerajik (Fenris), and Sleipner) (Fig. 3).

Within this broader acceleration phase, there was variability in the timing and evolution of speedup (Fig. 2, Fig. S1, Fig. S2a). Three dominant patterns emerge across the region. First, some glaciers accelerated continuously from early 2016, peaking around early 2020. Second, some glaciers accelerated in early 2016, then slowed or plateaued, particularly in 2017, before renewed acceleration in 2018, with speeds peaking in 2020. Third, some glaciers did not accelerate until around 2018, showing ice speed-up only in that later period. Examples of glaciers that exhibited continuous acceleration from 2016 to 2020 include Borgraven (Fig. 2a), Apuliliip Apusiia (Polaric) S (Fig. 2c), Apuseerajik (Fenris) (Fig. 2g) and Sleipner (Fig. 2i). Glaciers that showed early acceleration in 2016 followed by renewed acceleration in 2018 include Unaritit, Anorituup Kangerlua CN and CS (Fig. 2d,m,n). Glaciers where the onset of acceleration was delayed to 2018 include Kattilersorpia (Glacier de France) (Fig. 2f) and Avaqqat Kangerluat (Fig. 2o). K.J.V Steenstrup exhibits a combination of these behaviours, with initial acceleration in 2016 followed by a steeper increase after 2018.

https://doi.org/10.5194/egusphere-2026-5527
Preprint. Discussion started: 23 September 2026

Despite this variability, the region-wide pattern is coherent and represents some of the most rapid increases in ice speed ever observed, in just a few years. Overall, the observed speedup from 2016 to 2020 was much larger than anything on the record for most glaciers in the SE and CE Greenland region and marks a clear change in state from the muted change and in some cases slight deceleration observed in 2015 and the historical period prior to that (Fig. 2).

https://doi.org/10.5194/egusphere-2026-5527
Preprint. Discussion started: 23 September 2026

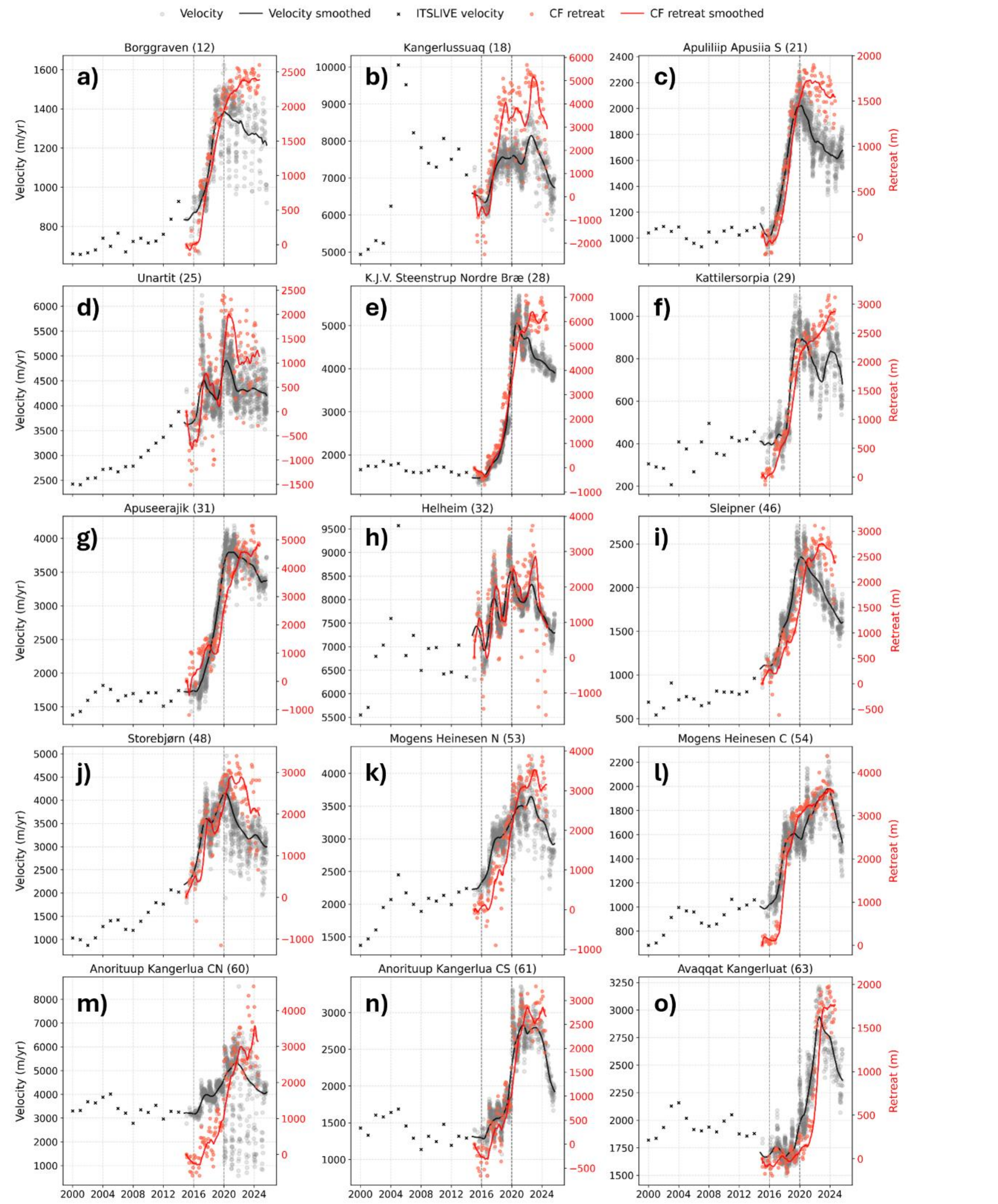

Figure 2 | Time series of ice-speed and calving-front change on 15 highlight glaciers in the SE and CE study region. The locations of these 15 glaciers are shown in Fig. 1, with glacier names and IDs shown above each plot. (a-o) Each time series shows the filtered monthly ice-speed observations derived from

https://doi.org/10.5194/egusphere-2026-5527
Preprint. Discussion started: 23 September 2026

Sentinel-1 intensity feature tracking (October 2014-August 2025) (light grey dots), the Kalman-smoothed ice velocity time series further smoothed with a 12-month rolling mean (solid black line), and historical annual ITSLIVE ice velocities (Gardner et al., 2025) plotted in June for each year from 2000 to 2014 (black dots). On the second y-axis we show calving front location change relative to the January 2015 front position (red dots), which combines Joughin and Black et al. (2022) (Black and Joughin, 2022) measurements (January 2015-December 2021) with our own manually delineated fronts (January 2022-September 2024). We show monthly calving front location change values for all glaciers except Helheim and Kangerlussuaq, which have weekly measurements for 2015–2021. The calving front change time series are interpolated to daily resolution and smoothed with a 12-month rolling mean (solid red line).

3.2.2 Ice speed peak

A consistent feature of the ice speed time series is that the speed peaked, rather than continuing to accelerate through to the end of our study period. On most glaciers we observe peak ice speeds clustering around late 2019 to early 2020 (Fig. S2b), although some glaciers including Mogens Heinsen N and C and Avaqqat Kangerluat (Fig. 2k, l, o) reached their peak ice speed slightly later (Fig. 2). The largest number of glaciers (six) reached their maximum speed in January 2020 (Fig. S2b), with twelve glaciers (18 % of those studied) reaching peak speeds within three months from November 2019 to January 2020, and one third of all glaciers reaching their peak speed in the 12-month window from June 2019 to June 2020. This clustering shows that late 2019 to early 2020 marked a turning point for glacier dynamics across the CE and SE coast of Greenland, with glaciers transitioning from the widespread acceleration phase to a new phase of widespread deceleration post-2020.

3.2.3 Deceleration phase (2020-2024)

Following the 2016 to 2020 ice speed acceleration phase, the SE and CE Greenland region entered a new widespread episode of glacier deceleration from January 2020 to January 2024 (Fig. 3b). During this period 45 out of the 66 glaciers in the region (68 %) showed a reduction in ice speed (Fig. 3b), with those that slowed doing so by an average of 15.5 %. Between 2020 and 2024, we observed the strongest percentage slowdown on Sortebrae (-84.9 ± 6 %), followed by Ikertivaq NN (-52.5 ± 4 %) and Danell Fjord (-47.3 ± 3 %). Only six glaciers increased in speed during this period with an average speed increase of 12.5 %, substantially less than the magnitude of the speed change observed in the earlier acceleration phase. The largest ice speed increases occurred on Avaqqat Kangerluat (23.8 ± 4 %) and Mogens Heinsen C (20.1 ± 5 %), while the other increases were more modest. Of the 43 glaciers that accelerated in the 2016-2020 period, 31 subsequently decelerated, eight showed no further significant change and only four continued to speed up (Fig. 3b).

3.2.4 Net change (2016-2024)

Although most glaciers slowed after 2020, the earlier accelerations were larger in magnitude, leading to a net increase in ice velocity across much of the CE and SE Greenland study region over the full 2016-2024 period (Fig. 1, Fig. 3c). When considering the complete record spanning both the acceleration and deceleration phases, 29 glaciers showed a net acceleration

https://doi.org/10.5194/egusphere-2026-5527
Preprint. Discussion started: 23 September 2026

with a 42.9 % increase in speed on average (Fig. 3c), and 8 glaciers increased their speed by over 50 %. In contrast, 17 glaciers experienced a net slowdown of 20.9 % on average, and 20 glaciers showed no overall change. Some slower-flowing glaciers showed particularly large relative speed increases, such as Kattilersorpia (Glacier de France) (105 %), however, given the slower absolute ice velocity these ice streams likely remain a small contributor to total ice discharge from the region. While we do observe seasonal ice speed variability on many glaciers on top of the multi-year acceleration and deceleration, this can appear much less pronounced or not visible at all in the time series due to the relatively smaller magnitude. Similarly, on most glaciers, the multi-year speedup signal is sustained throughout the winter months, often with no noticeable winter slowdown, indicating that the driver of this change is not only present during the summer months.

https://doi.org/10.5194/egusphere-2026-5527
Preprint. Discussion started: 23 September 2026

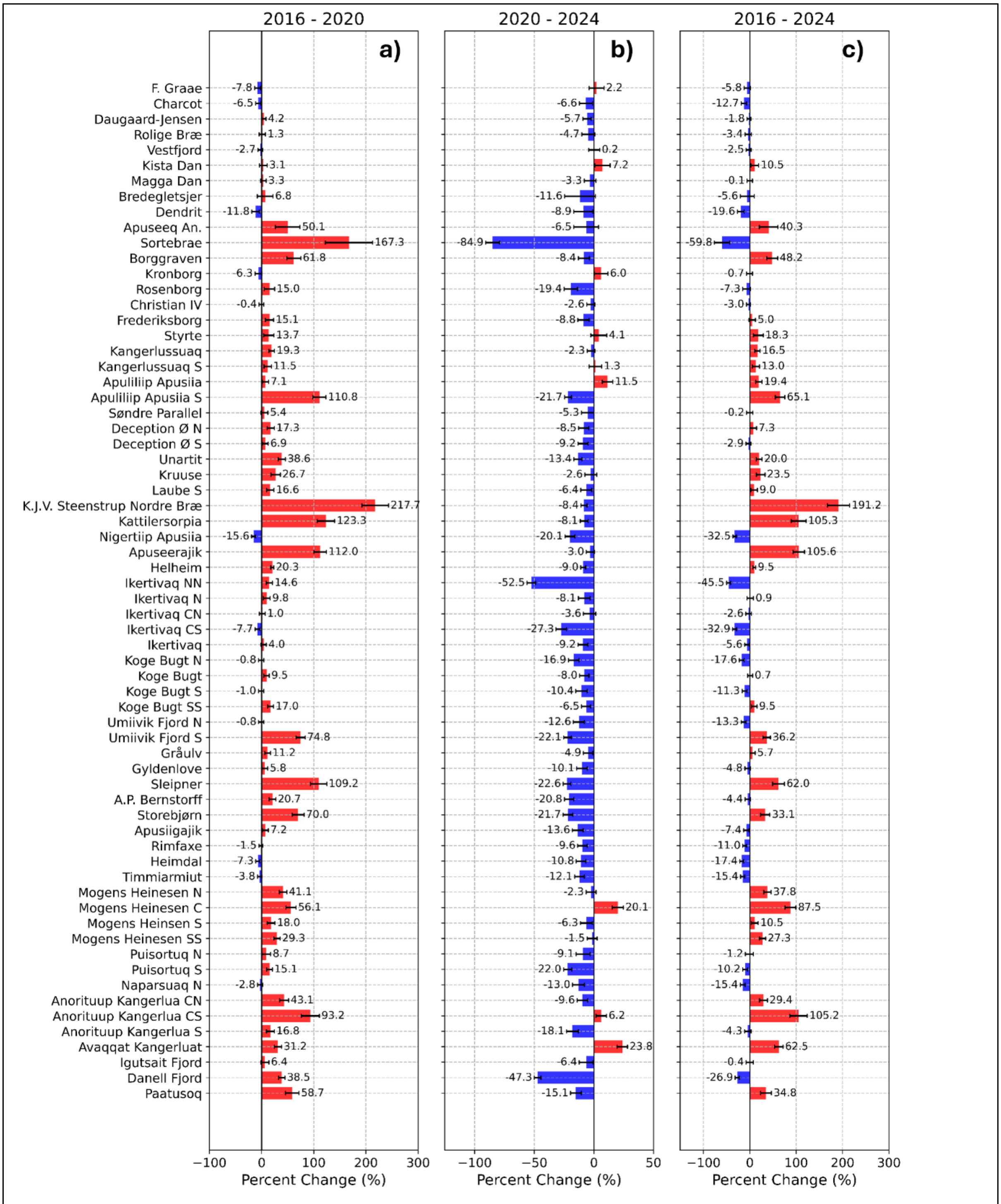

Figure 3 | Relative change in glacier speed from 2016–2020, 2020–2024, and 2016–2024, for all 66 glaciers in the study region. Percent change in glacier speed is shown for all 66 glaciers in the study region, ordered from north to south (ID 1-66), with positive (red bars) and negative (blue bars) speed change

https://doi.org/10.5194/egusphere-2026-5527
Preprint. Discussion started: 23 September 2026

both indicated. Percent change is computed from the mean monthly velocity values for each glacier between the two comparison months, and error bars (black bars) computed by propagating uncertainties in the monthly mean velocities. Panels show a) percent change between January 2016 and January 2020, b) percent change between January 2020 and January 2024, c) percent change between January 2016 and January 2024.

4 Discussion

4.1 Calving front change

In order to investigate the overall dynamic response of glaciers in the CE and SE Greenland study region we produced a time series of calving front location change on the 15 highlight glaciers over the full study period from 2015 to 2024 (Fig. 2). Our results show that overall, the calving front locations have changed on all 15 highlight glaciers in synchrony with the observed ice speed change episodes. During the main acceleration phase from 2016 to 2020 we observe a strong statistical correlation between the timing and magnitude of ice speedup and calving front retreat with an average Pearsons's coefficient of 0.907. Our observations show that all the highlight glaciers retreat between 2016 and 2020, but they then tend to undergo a change in behaviour in 2020, around the same time as the ice speed change peak occurred. On some glaciers like Apuliliip Apusiia (Polaric) S and Storebjorn the calving front readvances, on other glaciers the retreat plateaus or continues at a slower rate. The statistical correlation between the calving front change and ice velocity in the deceleration phase is much weaker after 2020 (Pearsons's coefficient of 0.154) due to this different behaviour. Calving front locations can only readvance at the rate at which glacier ice flows, so this may in part explain the poorer correlation and shows that the rate of ice flow acts as a control on the recovery period required for glacier readvance post dynamic activation, as observed in CE and SE Greenland. Over the full study period all glaciers underwent net retreat, with all but Helheim retreating more than 1 km and 10 glaciers retreating by over 2 km. The largest overall calving front retreat occurred on K.J.V Steenstrup (>6 km), followed by Apuseerajik (Fenris) which experienced just under 5 km of calving front retreat.

4.2 Environmental drivers of change

We considered what external drivers may have triggered the widespread episodes of ice dynamic variability observed across the SE and CE region of Greenland. The influence of ocean temperature on ice dynamics can be felt through its modulation of frontal ablation via submarine melt, calving and its influence on mélange rigidity (Wood et al., 2021). To investigate the potential role of ocean forcing we extracted average monthly ocean potential temperature from the Copernicus Marine Environment Monitoring Service (CMEMS) Arctic Ocean Physics Reanalysis (Arctic Ocean Physics Reanalysis, 2025) to assess how ocean conditions may have varied during the decade long study period (Fig. 4a). The results show that across all depths (0-300 m), ocean temperature anomalies transitioned from mostly negative before 2003 to predominantly positive afterward, indicating a long-term warming trend in the region. The data shows that a particularly strong positive ocean temperature anomaly appeared in the upper ocean (0 to ~50 m depth) in mid-2016, persisting until the end of that year, and peaking at almost +3 °C relative to the baseline at 6 m depth (Fig. 4b). This is over 1°C higher than any previous ocean temperature anomaly at that depth. In deeper water, the 2016 ocean temperature anomaly is present but weaker, reaching just under +0.5 °C at 200 m depth (Fig. 4c) which is comparable to other warm periods since 2003. The strongest warming at this depth occurred in 2018, when ocean temperature anomalies exceeded +1 °C, the largest anomaly recorded at that depth on the record.

The timing of these warm ocean temperature anomalies aligns closely with the onset of glacier speedup and calving front retreat (Fig. 4). The exceptionally warm surface waters in 2016 correspond to the initial, widespread glacier retreat and speed-up, while the deeper warm water anomaly in 2018 coincides with the second phase of ice speed acceleration seen on some glaciers. Ocean temperature anomalies notably decline in 2020 at both the surface and at depth, with surface waters remaining near zero or slightly negative and deeper waters showing modest warming that is within the normal range of variability since the early 2000's. This ocean temperature cooling in 2020 coincides with the widespread slowdown of glaciers in CE and SE Greenland, marking the end of the acceleration period. Overall, this result strongly suggests that ocean forcing played a driving role in triggering the observed ice dynamic change on the marine-terminating glaciers in SE and CE Greenland.

To assess climatic conditions in the region at the time of the observed ice dynamic variability, we extracted 2 m air temperature from the ERA5 reanalysis model (Hersbach et al., 2020; ERA5 monthly averaged data on single levels from 1940 to present, 2026) and calculated its associated anomaly (Fig. 4d). The results show that in correspondence with the long-term ocean temperature trends, the air temperature anomaly shifts from mostly negative to mostly positive air temperatures in the early 2000's. While there is a lot of very short-term air temperature variability that is likely caused by weather events, the 12-month rolling mean shows that 2016 stands out as a consistently warmer year (Fig. 4d), possibly causing the warm ocean surface temperature anomaly observed at this time (Fig. 4a). While air temperatures in 2016 are not substantially higher than earlier warm periods in 2010 or 2003, it does represent a sustained period of positive air temperature anomalies that could have influenced glaciological change in the region. Warmer air temperatures are known to influence glacier dynamics by increasing surface melt which lubricates the flow of ice, and this is likely the primary control on the seasonal ice speed variability we observe (Sundal et al., 2011). However, cold, freshwater runoff into the fjords can also impact ice-ocean interactions by affecting fjord overturning circulation, which enables warm ocean waters to reach the glacier front more effectively (Slater and Straneo, 2022; Straneo and Heimbach, 2013).

Both atmospheric and ocean forcing affect the formation and persistence of mélange and sea-ice in fjords and the surrounding region, both of which can exert a stabilising influence on glacier termini dampening the frequency of iceberg calving events (Howat et al., 2010; Walter et al., 2012). We extracted sea-ice concentration data along the continental shelf and calculated the associated anomaly (Fig. 4e), and while this dataset does not provide coverage in the small fjords that characterise this part of Greenland's coastline, it provides the best available data for assessing sea ice conditions during this period. The results

https://doi.org/10.5194/egusphere-2026-5527
Preprint. Discussion started: 23 September 2026

show a sustained negative sea ice concentration anomaly between 2016 and 2021, coinciding with the period of glacier acceleration and calving front retreat. Mélange can provide a consolidating effect on the glacier terminus, with reductions in coverage allowing more frequent calving and therefore retreat (Amundson et al., 2010, 2020) as previously observed at Kangerlussuaq (Bevan et al., 2019). Once retreat is initiated the bed geometry of the glacier will strongly influence how the glacier responds once forcing conditions change (Enderlin et al., 2013; Schoof, 2007), in part explaining the heterogeneity in response between neighbouring glaciers. Overall, the atmospheric and ocean conditions suggest that warm ocean waters and their influence on mélange and sea-ice conditions, were likely a key driver of the observed changes.

Local fjord geometry and bed topography impact how ocean temperature anomalies influence ice melt on individual glaciers, with features such as fjord depth, ridges, and sills controlling the properties of water reaching the glacier front (Batchelor et al., 2019; Wallis et al., 2023a). Southeast Greenland contains many deep fjords which allow warm Atlantic Water to access the glacier front and potentially trigger retreat (Millan et al., 2018; Palmer et al., 2025). Observations at K.J.V Steenstrup showed that access to deep, warm water likely contributed to its exceptional retreat and acceleration (Chudley et al., 2023). While similar processes may contribute to the speed up of other marine terminating glaciers along the coast, bathymetry remains very poorly resolved in many fjords in CE and SE Greenland (An et al., 2019), limiting our ability to quantify its role. Future studies should improve fjord and bed geometry mapping to better understand ocean circulation patterns within narrow fjord systems and to understand how routing of warm deep water reaches the ice sheet margin driving ice dynamic responses in this region.

https://doi.org/10.5194/egusphere-2026-5527
Preprint. Discussion started: 23 September 2026

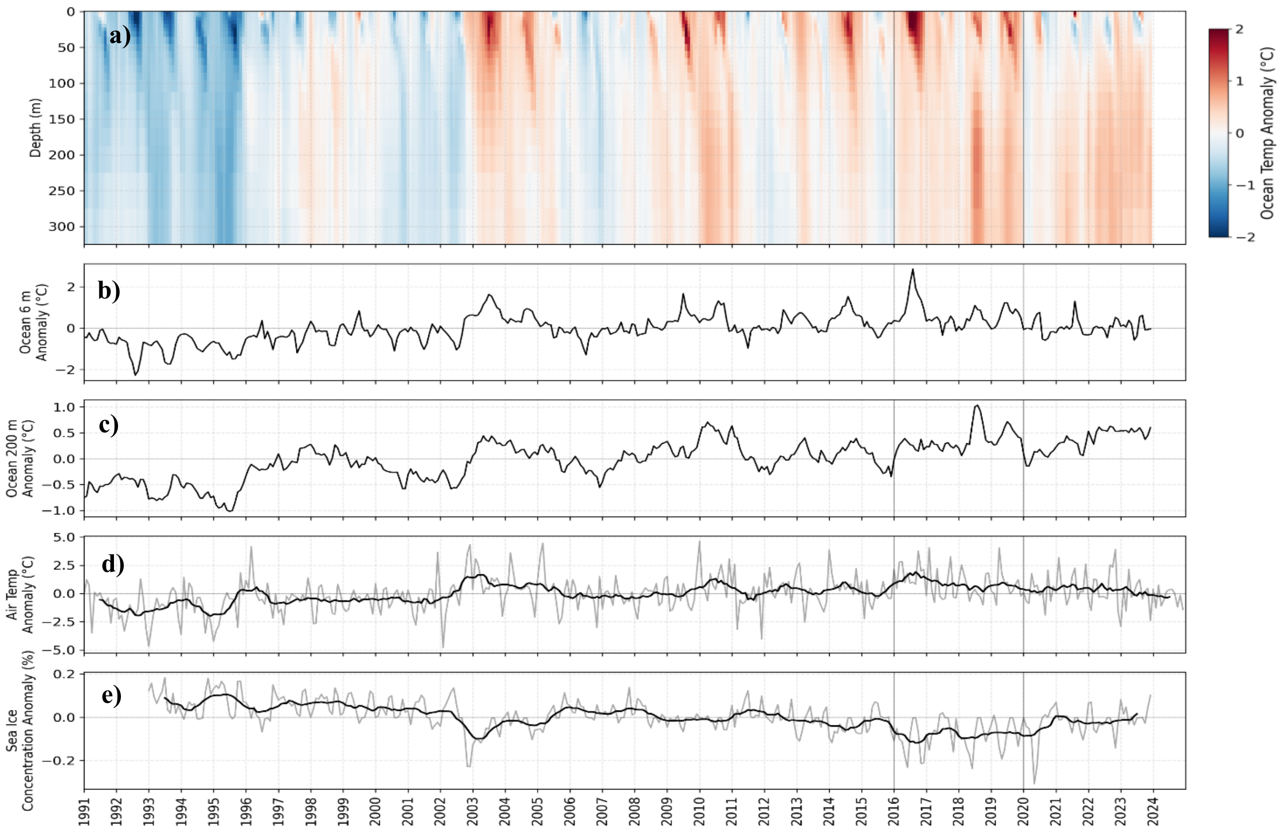

Figure 4 | Ocean, atmosphere temperature and sea-ice concentration anomalies in SE and CE Greenland. Average ocean temperature (Arctic Ocean Physics Reanalysis, 2025) and sea-ice concentration (Arctic Ocean Sea Ice Reanalysis, 2025) anomalies are extracted from the ocean portion of the dashed region in Fig. 1a while average ERA5 2 m air-temperature (ERA5 monthly averaged data on single levels from 1940 to present, 2026) anomalies are extracted over the full region outlined by the dashed line in Fig. 1a. a) Hovmoller plot of monthly ocean potential temperature anomalies from 0-300 m depth (1991-2024) relative to the long-term monthly climatology. b) Time series of 6 m ocean potential temperature anomalies (upper ocean). c) Time series of 200 m ocean potential temperature anomalies (Atlantic Water layer). d) Monthly 2 m air-temperature anomalies from ERA5. Grey line shows monthly values; black line shows 12-month rolling mean. e) Sea-ice concentration anomalies. Grey line shows monthly values; black line shows 12-month rolling mean. Vertical grey lines mark January 2016 and January 2020, corresponding to the onset and end of the widespread acceleration period (Fig's. 2-3).

4.3 Long term ice dynamic change

Our results show a clear, regionally coherent pattern of ice dynamic change across CE and SE Greenland from 2014 to 2025. Although previous studies have documented calving front retreat on a subset of these glaciers (Bevan et al., 2019; Brough et al., 2019, 2023) our results show that the signal was far more spatially extensive, affecting the majority of marine-terminating glaciers along the CE and SE Greenland coast. This behaviour initially resembles the ice speedup events characteristic of the

https://doi.org/10.5194/egusphere-2026-5527
Preprint. Discussion started: 23 September 2026

early 2000's (Moon et al., 2012) (Fig. 2), yet in many cases the change observed between 2016-2020 is much larger with several glaciers reaching their highest recorded speeds. Extension of the ice speed record on each glacier with historical data (Gardner et al., 2025) shows that on almost all 66 glaciers in our study region the 2020 ice speed peak is the fastest velocity measurement observed since at least 2000, often exceeding the early 2000's acceleration which was substantial in its own right (Fig. 2). Thirteen of the 15 highlight glaciers reach speeds which are often substantially higher than those seen before 2014, with Kangerlussuaq and Helheim (Fig. 2b, h) the only exceptions. The fact that a second, stronger, episode of widespread ice dynamic variability has now occurred in CE and SE Greenland suggests that glaciers in this region may be particularly susceptible to rapid, synchronous ice dynamic change (Christoffersen et al., 2011).

Although ocean driven changes appear central to the acceleration of CE and SE glaciers, the source of the ocean anomalies is less clear. This section of Greenland's coastline is influenced by both the East Greenland Current and the Irminger Current, which transport both cold polar waters and warm Atlantic-origin waters along the shelf (Sutherland et al., 2013). Moorings in the Fram Strait and upstream along the East Greenland Current, recorded warming and reduced sea ice since 2003, with a regime shift around 2015 (de Steur et al., 2023). These changes could have propagated along the coast and contributed to the extreme surface warming and reduced sea ice observed in our study region in 2016. Large scale atmospheric patterns such as the North Atlantic oscillation (NAO) and the state of the subpolar gyre can also influence the transport of warm water along the coast (Straneo and Heimbach, 2013; Wood et al., 2021). Future studies should investigate whether the dynamic variability we observe during this period in CE and SE Greenland expands even more widely to other parts of Greenland.

Despite the slowdown after 2020 most glaciers remain significantly faster than pre-2016 levels, indicating that the sea level contribution from this region of Greenland will have been elevated for approximately half a decade. In the long-term it remains uncertain whether glacier speeds will return to their original state following this change episode, or whether this represents a more permanent step change in regional ice dynamics. Either way, given projections of more extreme and less predictable atmospheric and ocean variability in Greenland in the coming decades (Fox-Kemper et al., 2023), it is essential to monitor and model this region of Greenland to monitor its ongoing and future response to environmental change.

5 Conclusion

We used over a decade of Sentinel-1 data to measure change in ice speed on 66 glaciers in central and southeast Greenland from 2014 and 2024 and observed a widespread pattern of synchronous ice dynamic change. Our results show widespread acceleration beginning in 2016 with speeds peaking in 2020, followed by lower-magnitude deceleration. This ice dynamic event was spatially extensive affecting nearly all the marine terminating glaciers in the region, and in many cases exceeding the magnitude of the historical speedup events of the early 2000's. Most glaciers in the SE and CE Greenland study region remain faster flowing than pre-2016 levels and will have experienced elevated ice discharge and sea level contribution for at least half a decade. Our results show that a significant ocean temperature anomaly occurred at the same time as the period of

https://doi.org/10.5194/egusphere-2026-5527
Preprint. Discussion started: 23 September 2026

acceleration and calving front retreat, which was the likely driver of the acceleration and subsequent slowdown. Overall, our findings highlight the sensitivity of this sector of Greenland, and its ability to respond rapidly to change. Future studies should monitor and model its evolution to better understand how future ocean and atmospheric variability may influence regional ice discharge and ice sheet mass balance.

Code and data availability

The original Copernicus Sentinel-1A/B data supporting this study can be freely downloaded from the Copernicus Data Space Ecosystem (https://dataspace.copernicus.eu/). Data generated in this study will be made freely and openly available on Zenodo on publication of this paper or on request by reviewers. Published datasets will include the ice speed and ice speed change map for the study region, ice speed timeseries for all 66 glaciers as shown in the supplementary material and calving front position shapefiles for the highlight glaciers.

Author contributions

MEE, AEH and TSS designed the study. MEE carried out the data analysis. RAWS, BJW and RR processed the underlying data. MEE wrote the manuscript with input from all authors.

Competing interests

The authors declare to have no competing interests.

Acknowledgements

The authors gratefully acknowledge the European Space Agency and the European Commission for the acquisition and availability of Copernicus Sentinel-1 data, which was retrieved from the Alaska Satellite Facility Distributed Active Archive Center (ASF DAAC). This work was undertaken on JASMIN, the UK's collaborative data analysis environment (https://www.jasmin.ac.uk) and AIRE, part of the High-Performance Computing facilities at the University of Leeds, UK. The ECMWF ERA5 datasets can be freely downloaded from the EU's Copernicus Climate Change Service Climate Data Store (ERA5: https://cds.climate.copernicus.eu/datasets/reanalysis-era5-single-levels?tab=overview). M. E. is funded by the Natural Environment Research Council (NERC) SENSE Centre for Doctoral Training (NE/T00939X/1). A.E.H is supported by ESA through the ARCTEX project (4000146172/24/I-KE), by NERC via the UK EO Climate Information Service (NE/X019071/1) project and by the Advanced Research + Invention Agency (ARIA) Forecasting Tipping Points Programme (GIANT project; SCOP-PR01-P028, GIANT Contribution No. GIANT-006).

https://doi.org/10.5194/egusphere-2026-5527
Preprint. Discussion started: 23 September 2026

References

Amundson, J. M., Fahnestock, M., Truffer, M., Brown, J., Lüthi, M. P., and Motyka, R. J.: Ice mélange dynamics and implications for terminus stability, Jakobshavn Isbræ, Greenland, Journal of Geophysical Research: Earth Surface, 115, https://doi.org/10.1029/2009JF001405, 2010.

Amundson, J. M., Kienholz, C., Hager, A. O., Jackson, R. H., Motyka, R. J., Nash, J. D., and Sutherland, D. A.: Formation, flow and break-up of ephemeral ice mélange at LeConte Glacier and Bay, Alaska, Journal of Glaciology, 66, 577–590, https://doi.org/10.1017/jog.2020.29, 2020.

An, L., Rignot, E., Chauche, N., Holland, D. M., Holland, D., Jakobsson, M., Kane, E., Wood, M., Klaucke, I., Morlighem, M., Velicogna, I., Weinrebe, W., and Willis, J. K.: Bathymetry of Southeast Greenland From Oceans Melting Greenland (OMG) Data, Geophysical Research Letters, 46, 11197–11205, https://doi.org/10.1029/2019GL083953, 2019.

Arctic Ocean Physics Reanalysis. E.U. Copernicus Marine Service Information (CMEMS). Marine Data Store (MDS). DOI: 10.48670/moi-00007 (Accessed on 16 07 2026), 2025.

Arctic Ocean Sea Ice Reanalysis. E.U. Copernicus Marine Service Information (CMEMS). Marine Data Store (MDS). DOI: 10.48670/mds-00336 (Accessed on 16 07 2026), 2025.

Batchelor, C. L., Dowdeswell, J. A., Rignot, E., and Millan, R.: Submarine Moraines in Southeast Greenland Fjords Reveal Contrasting Outlet-Glacier Behavior since the Last Glacial Maximum, Geophysical Research Letters, 46, 3279–3286, https://doi.org/10.1029/2019GL082556, 2019.

Bevan, S. L., Luckman, A. J., Benn, D. I., Cowton, T., and Todd, J.: Impact of warming shelf waters on ice mélange and terminus retreat at a large SE Greenland glacier, The Cryosphere, 13, 2303–2315, https://doi.org/10.5194/tc-13-2303-2019, 2019.

Bhattacharya, S., Charonko, J. J., and Vlachos, P. P.: Particle image velocimetry (PIV) uncertainty quantification using moment of correlation (MC) plane, Meas. Sci. Technol., 29, 115301, https://doi.org/10.1088/1361-6501/aadfb4, 2018.

Black, T. and Joughin, I.: MEaSUREs Weekly to Monthly Greenland Outlet Glacier Terminus Positions from Sentinel-1 Mosaics, Version 1, https://doi.org/10.5067/DGBOSSIULSTD, 2022.

Black, T. E. and Joughin, I.: Weekly to monthly terminus variability of Greenland's marine-terminating outlet glaciers, The Cryosphere, 17, 1–13, https://doi.org/10.5194/tc-17-1-2023, 2023.

van den Broeke, M. R., Enderlin, E. M., Howat, I. M., Kuipers Munneke, P., Noël, B. P. Y., van de Berg, W. J., van Meijgaard, E., and Wouters, B.: On the recent contribution of the Greenland ice sheet to sea level change, The Cryosphere, 10, 1933–1946, https://doi.org/10.5194/tc-10-1933-2016, 2016.

Brough, S., Carr, J. R., Ross, N., and Lea, J. M.: Exceptional Retreat of Kangerlussuaq Glacier, East Greenland, Between 2016 and 2018, Front. Earth Sci., 7, https://doi.org/10.3389/feart.2019.00123, 2019.

Brough, S., Carr, J. R., Ross, N., and Lea, J. M.: Ocean-Forcing and Glacier-Specific Factors Drive Differing Glacier Response Across the 69°N Boundary, East Greenland, Journal of Geophysical Research: Earth Surface, 128, e2022JF006857, https://doi.org/10.1029/2022JF006857, 2023.

Choi, Y., Morlighem, M., Rignot, E., and Wood, M.: Ice dynamics will remain a primary driver of Greenland ice sheet mass loss over the next century, Commun Earth Environ, 2, 26, https://doi.org/10.1038/s43247-021-00092-z, 2021.

https://doi.org/10.5194/egusphere-2026-5527
Preprint. Discussion started: 23 September 2026

Christoffersen, P., Mugford, R. I., Heywood, K. J., Joughin, I., Dowdeswell, J. A., Syvitski, J. P. M., Luckman, A., and Benham, T. J.: Warming of waters in an East Greenland fjord prior to glacier retreat: mechanisms and connection to large-scale atmospheric conditions, The Cryosphere, 5, 701–714, https://doi.org/10.5194/tc-5-701-2011, 2011.

Chudley, T. R., Howat, I. M., King, M. D., and Negrete, A.: Atlantic water intrusion triggers rapid retreat and regime change at previously stable Greenland glacier, Nat Commun, 14, 2151, https://doi.org/10.1038/s41467-023-37764-7, 2023.

Copernicus Climate Change Service: ERA5 monthly averaged data on single levels from 1940 to present, https://doi.org/10.24381/cds.f17050d7, 2023.

Copernicus Climate Change Service, Climate Data Store: Ice sheet velocity for Antarctica and Greenland derived from satellite observations. Copernicus Climate Change Service (C3S) Climate Data Store (CDS), DOI: 10.24381/cds.0b96b838 (date of last access 16-07-2026), 2020.

Davison, B. J., Hogg, A. E., Moffat, C., Meredith, M. P., and Wallis, B. J.: Widespread increase in discharge from west Antarctic Peninsula glaciers since 2018, The Cryosphere, 18, 3237–3251, https://doi.org/10.5194/tc-18-3237-2024, 2024.

Enderlin, E. M., Howat, I. M., and Vieli, A.: High sensitivity of tidewater outlet glacier dynamics to shape, The Cryosphere, 7, 1007–1015, https://doi.org/10.5194/tc-7-1007-2013, 2013.

Enderlin, E. M., Howat, I. M., Jeong, S., Noh, M.-J., van Angelen, J. H., and van den Broeke, M. R.: An improved mass budget for the Greenland ice sheet, Geophysical Research Letters, 41, 866–872, https://doi.org/10.1002/2013GL059010, 2014.

Fox-Kemper, B., H.T. Hewitt, C. Xiao, G. Aðalgeirsdóttir, S.S. Drijfhout, T.L. Edwards, N.R. Golledge, M. Hemer, R.E. Kopp, G. Krinner, A. Mix, D. Notz, S. Nowicki, I.S. Nurhati, L. Ruiz, J.-B. Sallée, A.B.A. Slangen, and Y. Yu, 2021: Ocean, Cryosphere and Sea Level Change. In *Climate Change 2021: The Physical Science Basis. Contribution of Working Group I to the Sixth Assessment Report of the Intergovernmental Panel on Climate Change* [Masson-Delmotte, V., P. Zhai, A. Pirani, S.L. Connors, C. Péan, S. Berger, N. Caud, Y. Chen, L. Goldfarb, M.I. Gomis, M. Huang, K. Leitzell, E. Lonnoy, J.B.R. Matthews, T.K. Maycock, T. Waterfield, O. Yelekçi, R. Yu, and B. Zhou (eds.)]. Cambridge University Press, Cambridge, United Kingdom and New York, NY, USA, pp. 1211–1362, doi: 10.1017/9781009157896.011.

Gardner, A., Fahnestock, M., Greene, C. A., Kennedy, J. H., Liukis, M., Lopez, L. A., and Scambos, T.: MEASURES ITS_LIVE Regional Glacier and Ice Sheet Surface Velocities, Version 2, https://doi.org/10.5067/JQ6337239C96, 2024.

Gardner, A. S., Greene, C. A., Kennedy, J. H., Fahnestock, M. A., Liukis, M., López, L. A., Lei, Y., Scambos, T. A., and Dehecq, A.: ITS_LIVE global glacier velocity data in near-real time, The Cryosphere, 19, 3517–3533, https://doi.org/10.5194/tc-19-3517-2025, 2025.

Gerrish, L.: The coastline of Kalaallit Nunaat/ Greenland available as a shapefile and geopackage, covering the main land and islands, with glacier fronts updated as of 2017. (1.0), https://doi.org/10.5285/8CECDE06-8474-4B58-A9CB-B820FA4C9429, 2020.

Hersbach, H., Bell, B., Berrisford, P., Hirahara, S., Horányi, A., Muñoz-Sabater, J., Nicolas, J., Peubey, C., Radu, R., Schepers, D., Simmons, A., Soci, C., Abdalla, S., Abellan, X., Balsamo, G., Bechtold, P., Biavati, G., Bidlot, J., Bonavita, M., De Chiara, G., Dahlgren, P., Dee, D., Diamantakis, M., Dragani, R., Flemming, J., Forbes, R., Fuentes, M., Geer, A., Haimberger, L., Healy, S., Hogan, R. J., Hólm, E., Janisková, M., Keeley, S., Laloyaux, P., Lopez, P., Lupu, C., Radnoti, G., de Rosnay, P., Rozum, I., Vamborg, F., Villaume, S., and Thépaut, J.-N.: The ERA5 global reanalysis, Quarterly Journal of the Royal Meteorological Society, 146, 1999–2049, https://doi.org/10.1002/qj.3803, 2020.

https://doi.org/10.5194/egusphere-2026-5527
Preprint. Discussion started: 23 September 2026

Howat, I. M., Joughin, I., and Scambos, T. A.: Rapid Changes in Ice Discharge from Greenland Outlet Glaciers, Science, 315, 1559–1561, https://doi.org/10.1126/science.1138478, 2007.

Howat, I. M., Box, J. E., Ahn, Y., Herrington, A., and McFadden, E. M.: Seasonal variability in the dynamics of marine-terminating outlet glaciers in Greenland, Journal of Glaciology, 56, 601–613, https://doi.org/10.3189/002214310793146232, 2010.

King, M. D., Howat, I. M., Candela, S. G., Noh, M. J., Jeong, S., Noël, B. P. Y., van den Broeke, M. R., Wouters, B., and Negrete, A.: Dynamic ice loss from the Greenland Ice Sheet driven by sustained glacier retreat, Commun Earth Environ, 1, 1, https://doi.org/10.1038/s43247-020-0001-2, 2020.

Lea, J. M.: The Google Earth Engine Digitisation Tool (GEEDiT) and the Margin change Quantification Tool (MaQiT) – simple tools for the rapid mapping and quantification of changing Earth surface margins, Earth Surface Dynamics, 6, 551–561, https://doi.org/10.5194/esurf-6-551-2018, 2018.

Lemos, A., Shepherd, A., McMillan, M., Hogg, A. E., Hatton, E., and Joughin, I.: Ice velocity of Jakobshavn Isbræ, Petermann Glacier, Nioghalvfjerdsfjorden, and Zachariæ Isstrøm, 2015–2017, from Sentinel 1-a/b SAR imagery, The Cryosphere, 12, 2087–2097, https://doi.org/10.5194/tc-12-2087-2018, 2018.

Liu, J., Enderlin, E., Marshall, H.-P., and Khalil, A.: Synchronous Retreat of Southeast Greenland's Peripheral Glaciers, Geophysical Research Letters, 49, e2022GL097756, https://doi.org/10.1029/2022GL097756, 2022.

Mankoff, K. D., Solgaard, A., Colgan, W., Ahlstrøm, A. P., Khan, S. A., and Fausto, R. S.: Greenland Ice Sheet solid ice discharge from 1986 through March 2020, Earth System Science Data, 12, 1367–1383, https://doi.org/10.5194/essd-12-1367-2020, 2020.

Millan, R., Rignot, E., Mouginot, J., Wood, M., Bjørk, A. A., and Morlighem, M.: Vulnerability of Southeast Greenland Glaciers to Warm Atlantic Water From Operation IceBridge and Ocean Melting Greenland Data, Geophysical Research Letters, 45, 2688–2696, https://doi.org/10.1002/2017GL076561, 2018.

Moon, T., Joughin, I., Smith, B., and Howat, I.: 21st-Century Evolution of Greenland Outlet Glacier Velocities, Science, 336, 576–578, https://doi.org/10.1126/science.1219985, 2012.

Mouginot, J., Rignot, E., Bjørk, A. A., van den Broeke, M., Millan, R., Morlighem, M., Noël, B., Scheuchl, B., and Wood, M.: Forty-six years of Greenland Ice Sheet mass balance from 1972 to 2018, Proceedings of the National Academy of Sciences, 116, 9239–9244, https://doi.org/10.1073/pnas.1904242116, 2019a.

Mouginot, J., Rignot, E., Bjørk, A. A., van den Broeke, M., Millan, R., Morlighem, M., Noël, B., Scheuchl, B., and Wood, M.: Forty-six years of Greenland Ice Sheet mass balance from 1972 to 2018, Proceedings of the National Academy of Sciences, 116, 9239–9244, https://doi.org/10.1073/pnas.1904242116, 2019b.

Nagler, T., Rott, H., Hetzenecker, M., Wuite, J., and Potin, P.: The Sentinel-1 Mission: New Opportunities for Ice Sheet Observations, Remote Sensing, 7, 9371–9389, https://doi.org/10.3390/rs70709371, 2015.

Otosaka, I. N., Shepherd, A., Ivins, E. R., Schlegel, N.-J., Amory, C., van den Broeke, M. R., Horwath, M., Joughin, I., King, M. D., Krinner, G., Nowicki, S., Payne, A. J., Rignot, E., Scambos, T., Simon, K. M., Smith, B. E., Sørensen, L. S., Velicogna, I., Whitehouse, P. L., A, G., Agosta, C., Ahlstrøm, A. P., Blazquez, A., Colgan, W., Engdahl, M. E., Fettweis, X., Forsberg, R., Gallée, H., Gardner, A., Gilbert, L., Gourmelen, N., Groh, A., Gunter, B. C., Harig, C., Helm, V., Khan, S. A., Kittel, C., Konrad, H., Langen, P. L., Lecavalier, B. S., Liang, C.-C., Loomis, B. D., McMillan, M., Melini, D., Mernild, S. H., Mottram, R., Mouginot, J., Nilsson, J., Noël, B., Pattle, M. E., Peltier, W. R., Pie, N., Roca, M., Sasgen, I., Save, H. V., Seo, K.-W., Scheuchl, B., Schrama, E. J. O., Schröder, L., Simonsen, S. B., Slater, T., Spada, G., Sutterley, T. C., Vishwakarma, B. D., van Wessem, J. M., Wiese, D., van der Wal, W., and Wouters, B.: Mass balance of the Greenland and Antarctic ice sheets from 1992 to 2020, Earth System Science Data, 15, 1597–1616, https://doi.org/10.5194/essd-15-1597-2023, 2023.

Palmer, S., Kirkwood, C., Luo, C., and Morlighem, M.: A quantile regression forest estimate of Greenland's subglacial topography, Journal of Glaciology, 71, e115, https://doi.org/10.1017/jog.2025.10071, 2025.

Porter, C., Howat, I., Noh, M.-J., Husby, E., Khuvis, S., Danish, E., Tomko, K., Gardiner, J., Negrete, A., Yadav, B., Klassen, J., Kelleher, C., Cloutier, M., Bakker, J., Enos, J., Arnold, G., Bauer, G., and Morin, P.: ArcticDEM - Mosaics, Version 4.1, https://doi.org/10.7910/DVN/3VDC4W, 2023.

Rott, H., Wuite, J., De Rydt, J., Gudmundsson, G. H., Floricioiu, D., and Rack, W.: Impact of marine processes on flow dynamics of northern Antarctic Peninsula outlet glaciers, Nat Commun, 11, 2969, https://doi.org/10.1038/s41467-020-16658-y, 2020.

Schoof, C.: Ice sheet grounding line dynamics: Steady states, stability, and hysteresis, Journal of Geophysical Research: Earth Surface, 112, https://doi.org/10.1029/2006JF000664, 2007.

Seale, A., P. Christoffersen, R. I. Mugford, and M. O'Leary: Ocean forcing of the Greenland Ice Sheet: Calving fronts and patterns of retreat identified by automatic satellite monitoring of eastern outlet glaciers, *J. Geophys. Res.*, 116, F03013, DOI :10.1029/2010JF001847, 2011.

Selley, H. L., Hogg, A. E., Cornford, S., Dutrieux, P., Shepherd, A., Wuite, J., Floricioiu, D., Kusk, A., Nagler, T., Gilbert, L., Slater, T., and Kim, T.-W.: Widespread increase in dynamic imbalance in the Getz region of Antarctica from 1994 to 2018, Nat Commun, 12, 1133, https://doi.org/10.1038/s41467-021-21321-1, 2021.

Shepherd, A., Ivins, E., Rignot, E., Smith, B., van den Broeke, M., Velicogna, I., Whitehouse, P., Briggs, K., Joughin, I., Krinner, G., Nowicki, S., Payne, T., Scambos, T., Schlegel, N., A, G., Agosta, C., Ahlstrøm, A., Babonis, G., Barletta, V. R., Bjørk, A. A., Blazquez, A., Bonin, J., Colgan, W., Csatho, B., Cullather, R., Engdahl, M. E., Felikson, D., Fettweis, X., Forsberg, R., Hogg, A. E., Gallee, H., Gardner, A., Gilbert, L., Gourmelen, N., Groh, A., Gunter, B., Hanna, E., Harig, C., Helm, V., Horvath, A., Horwath, M., Khan, S., Kjeldsen, K. K., Konrad, H., Langen, P. L., Lecavalier, B., Loomis, B., Luthcke, S., McMillan, M., Melini, D., Mernild, S., Mohajerani, Y., Moore, P., Mottram, R., Mouginot, J., Moyano, G., Muir, A., Nagler, T., Nield, G., Nilsson, J., Noël, B., Otosaka, I., Pattle, M. E., Peltier, W. R., Pie, N., Rietbroek, R., Rott, H., Sandberg Sørensen, L., Sasgen, I., Save, H., Scheuchl, B., Schrama, E., Schröder, L., Seo, K.-W., Simonsen, S. B., Slater, T., Spada, G., Sutterley, T., Talpe, M., Tarasov, L., van de Berg, W. J., van der Wal, W., van Wessem, M., Vishwakarma, B. D., Wiese, D., Wilton, D., Wagner, T., Wouters, B., Wuite, J., and The IMBIE Team: Mass balance of the Greenland Ice Sheet from 1992 to 2018, Nature, 579, 233–239, https://doi.org/10.1038/s41586-019-1855-2, 2020.

Slater, D. A. and Straneo, F.: Submarine melting of glaciers in Greenland amplified by atmospheric warming, Nat. Geosci., 15, 794–799, https://doi.org/10.1038/s41561-022-01035-9, 2022.

Solgaard, A., Kusk, A., Merryman Boncori, J. P., Dall, J., Mankoff, K. D., Ahlstrøm, A. P., Andersen, S. B., Citterio, M., Karlsson, N. B., Kjeldsen, K. K., Korsgaard, N. J., Larsen, S. H., and Fausto, R. S.: Greenland ice velocity maps from the PROMICE project, Earth System Science Data, 13, 3491–3512, https://doi.org/10.5194/essd-13-3491-2021, 2021.

de Steur, L., Sumata, H., Divine, D. V., Granskog, M. A., and Pavlova, O.: Upper ocean warming and sea ice reduction in the East Greenland Current from 2003 to 2019, Commun Earth Environ, 4, 261, https://doi.org/10.1038/s43247-023-00913-3, 2023.

https://doi.org/10.5194/egusphere-2026-5527
Preprint. Discussion started: 23 September 2026

Straneo, F. and Heimbach, P.: North Atlantic warming and the retreat of Greenland's outlet glaciers, Nature, 504, 36–43, https://doi.org/10.1038/nature12854, 2013.

Strozzi, T., Luckman, A., Murray, T., Wegmuller, U., and Werner, C. L.: Glacier motion estimation using SAR offset-tracking procedures, IEEE Transactions on Geoscience and Remote Sensing, 40, 2384–2391, https://doi.org/10.1109/TGRS.2002.805079, 2002a.

Strozzi, T., Luckman, A., Murray, T., Wegmuller, U., and Werner, C. L.: Glacier motion estimation using SAR offset-tracking procedures, IEEE Transactions on Geoscience and Remote Sensing, 40, 2384–2391, https://doi.org/10.1109/TGRS.2002.805079, 2002b.

Sundal, A. V., Shepherd, A., Nienow, P., Hanna, E., Palmer, S., and Huybrechts, P.: Melt-induced speed-up of Greenland ice sheet offset by efficient subglacial drainage, Nature, 469, 521–524, https://doi.org/10.1038/nature09740, 2011.

Sutherland, D. A., Straneo, F., Stenson, G. B., Davidson, F. J. M., Hammill, M. O., and Rosing-Asvid, A.: Atlantic water variability on the SE Greenland continental shelf and its relationship to SST and bathymetry, Journal of Geophysical Research: Oceans, 118, 847–855, https://doi.org/10.1029/2012JC008354, 2013.

Wallis, B. J., Hogg, A. E., Meredith, M. P., Close, R., Hardy, D., McMillan, M., Wuite, J., Nagler, T., and Moffat, C.: Ocean warming drives rapid dynamic activation of marine-terminating glacier on the west Antarctic Peninsula, Nat Commun, 14, 7535, https://doi.org/10.1038/s41467-023-42970-4, 2023a.

Wallis, B. J., Hogg, A. E., van Wessem, J. M., Davison, B. J., and van den Broeke, M. R.: Widespread seasonal speed-up of west Antarctic Peninsula glaciers from 2014 to 2021, Nat. Geosci., 16, 231–237, https://doi.org/10.1038/s41561-023-01131-4, 2023b.

Walter, J. I., Box, J. E., Tulaczyk, S., Brodsky, E. E., Howat, I. M., Ahn, Y., and Brown, A.: Oceanic mechanical forcing of a marine-terminating Greenland glacier, Annals of Glaciology, 53, 181–192, https://doi.org/10.3189/2012AoG60A083, 2012.

Wood, M., Rignot, E., Fenty, I., An, L., Bjørk, A., van den Broeke, M., Cai, C., Kane, E., Menemenlis, D., Millan, R., Morlighem, M., Mouginot, J., Noël, B., Scheuchl, B., Velicogna, I., Willis, J. K., and Zhang, H.: Ocean forcing drives glacier retreat in Greenland, Science Advances, 7, eaba7282, https://doi.org/10.1126/sciadv.aba7282, 2021.